TWO-DIMENSIONAL NMR FOR THREE-DIMENSIONAL STRUCTURE OF NUCLEIC ACIDS: NEW TECHNIQUES AND NOVEL RESULTS

R. V. HOSUR

Chemical Physics Group, Tata Institute of Fundamental Research, Homi Bhabha Road, Bombay 400 005, India.

ABSTRACT

The principles and the variety of two-dimensional (2D) NMR techniques useful for structure determination of nucleic acids have been described. Three new techniques namely, SUPERCOSY, *J*-scaled COSY and COSS which have been recently developed to overcome the problems of sensitivity and resolution have been described in greater detail. The strategies of resonance assignments and structure determination of nucleic acids have been discussed and the experimental results on four oligonucleotides longer than a complete turn of nucleic acid helix have been presented. The data indicate O1′-endo sugar geometry in a majority of the nucleotide units in two oligonucleotides namely, *d*-GAATTCGAATTC and *d*-GAATTCCCGAATTC.

INTRODUCTION

NUCLEIC acids are the most fundamental molecules of life. Deoxyribonucleic acid (DNA) is primarily a storehouse of genetic information and this is expressed in living systems in the form of proteins which carry out the various functions of life. The process of expression involves a complex interplay between proteins and nucleic acids and involves specific recognition of short segments of nucleic acids by certain proteins. At the molecular level, the interaction between the two kinds of molecules are responsible for such specific recognition phenomena. It is obvious that the three-dimensional (3D) structures of the individual molecules play a crucial role in deciding the nature of the interactions and thus in recognition mechanisms. This also holds good in a variety of drug-nucleic acid interactions.

Nuclear magnetic resonance (NMR) has proved to be a very valuable tool for determination of molecular conformations in aqueous solutions[1]. In the past, NMR parameters such as chemical shifts, 3-bond ^1H–^1H coupling constants have been used in conjunction with potential energy calculations[2–5] to derive information about dynamics and preferred conformations in a variety of short nucleic acid fragments. The lengths were restricted to about 2–4 nucleotide units owing to extensive overlap problems in the NMR spectra of larger molecules. In the last few years, the advent of 2D NMR spectroscopy has changed the scene and it is now possible to work with nucleic acid fragments as large as 10–20 nucleotide units. The information derivable from 2D NMR spectra is also substantially higher than that from the conventional 1D spectra. The field of 2D NMR spectroscopy and its application has been expanding at a very rapid pace. Better pulse sequences are being invented and 3D structures of larger and larger molecules are being determined[6–10]. We have been working on both these fronts, one complementing the other. The aim of this article is to review the work carried out in both these areas in our laboratory. In this connection, we discuss below the important 2D NMR techniques briefly and then describe their use in resonance assignments and structure determination of nucleic acid fragments.

TWO-DIMENSIONAL NMR TECHNIQUES

2D NMR is basically an extension of the 1D Fourier-transform (FT) NMR technique. A 2D spectrum has two frequency axes (ω_1, ω_2) and the

intensities are represented along the third axis. Thus each peak in a 2D spectrum occupies volume as against an area in the 1D spectrum. The two frequencies in a 2D spectrum are generated by Fourier transformation of a time domain data matrix of two independent time variables t_1 and t_2.

$$s(t_1, t_2) \rightarrow S\ (\omega_1, \omega_2).$$

The two time variables are generated by segmentation of the conventional time axis of the FT NMR experiment. The period t_1 is called the evolution period, while the period t_2 is termed as the detection period. It is only during the latter that the data is collected. The purpose of the variety of 2D NMR techniques is to establish a correlation between the behaviour of the spin system during the two periods. This is achieved by a so-called mixing period which separates the detection period from the evolution period. The mixing period is a constant time period while the evolution and detection periods vary in time i.e. experiments are repeated for systematically increasing values of t_1 and data is collected in each case as a function of t_2. In general, the spin systems evolve under different Hamiltonians in each of these periods. Among the variety of 2D NMR techniques, the pulse schemes of those which are useful for structure determination of nucleic acids are shown in figure 1.

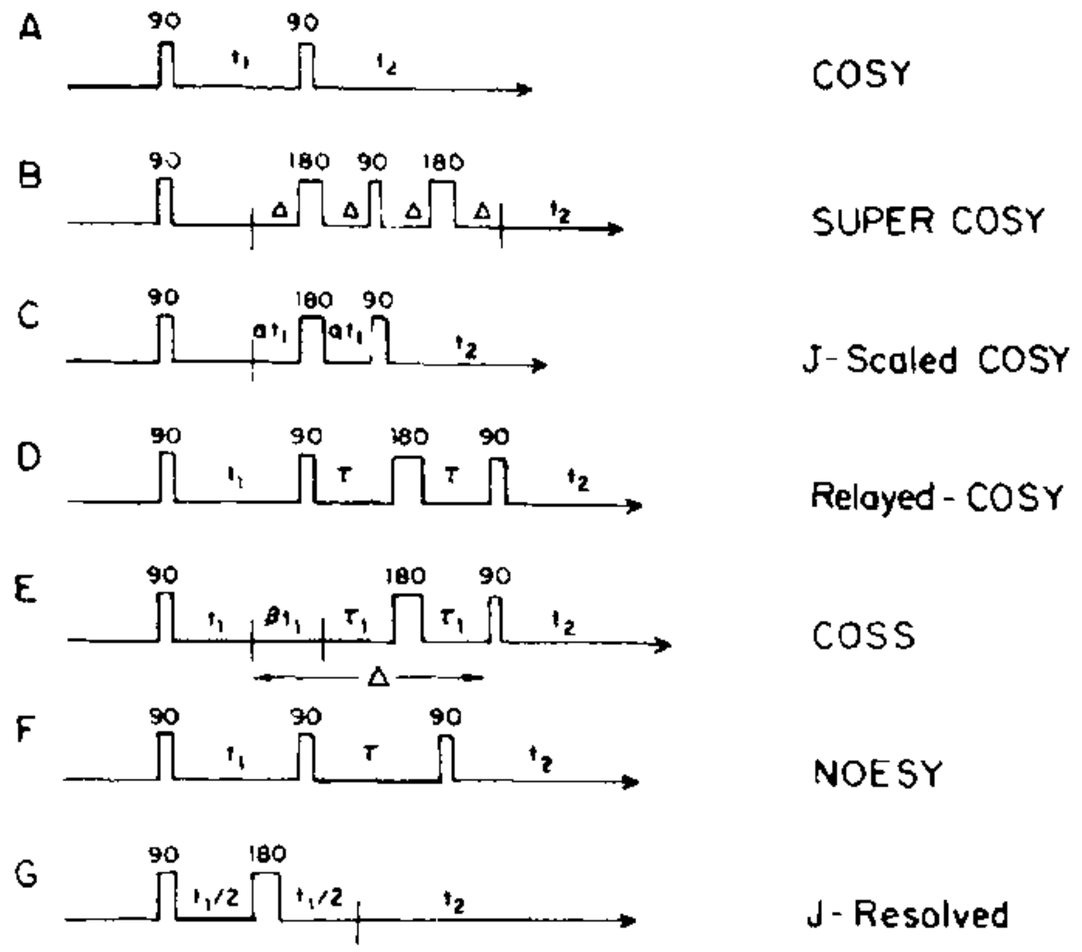

Figure 1. Pulse schemes of various 2D-NMR techniques. Δ, τ are fixed time periods. In COSS, τ_1 is variable which changes with t_1 to keep Δ constant. α and β are constants which determine J-scaling factor $(1+2\alpha)$ and shift scaling factor $(1+\beta)$ respectively.

Pulse scheme A (COSY) is the simplest among all the 2D experiments[11-12]. The first 90° pulse creates transverse magnetization. During the evolution period, the various spins are labelled by their characteristic frequencies. The second 90° pulse acts as a mixing pulse and transfers magnetization between J-coupled spins in the system. This establishes a correlation between J-coupled spins and is reflected in the spectrum as an off-diagonal peak. Some spins do not exchange magnetization and these spins give rise to peaks along the diagonal in the 2D COSY spectrum. Both diagonal and off-diagonal or cross peaks have multiplet structures characteristic of the spins from which they originate. A typical COSY spectrum for a two spin system is shown in figure 2a. The spectrum has a symmetry and the two triangles separated by the diagonal have the same information. The + and − signs indicate positive and negative peaks. The separation between these components is equal to the coupling constant J between the two spins. The COSY spectrum is useful for identification of coupling networks in a given spin system.

Figure 2a indicates that the diagonal peaks have a net integrated intensity, whereas the cross peaks possess a zero-integrated intensity. This feature of the cross peaks results in poor intensities under conditions of low resolution in the spectrum. For the same reason, it is hard to observe small-J correlations in the COSY spectrum. On the other hand, the diagonal peak components co-add and produce very strong peaks. The low intensity of the cross peaks which actually carry the coupling information is of course highly undesirable. The low intensity ratio of cross peak: diagonal peak also gives rise to 'dynamic range' problems in the 2D spectrum.

Pulse scheme B termed as SUPERCOSY[13] is an improvement over the COSY spectrum and overcomes some of the problems mentioned

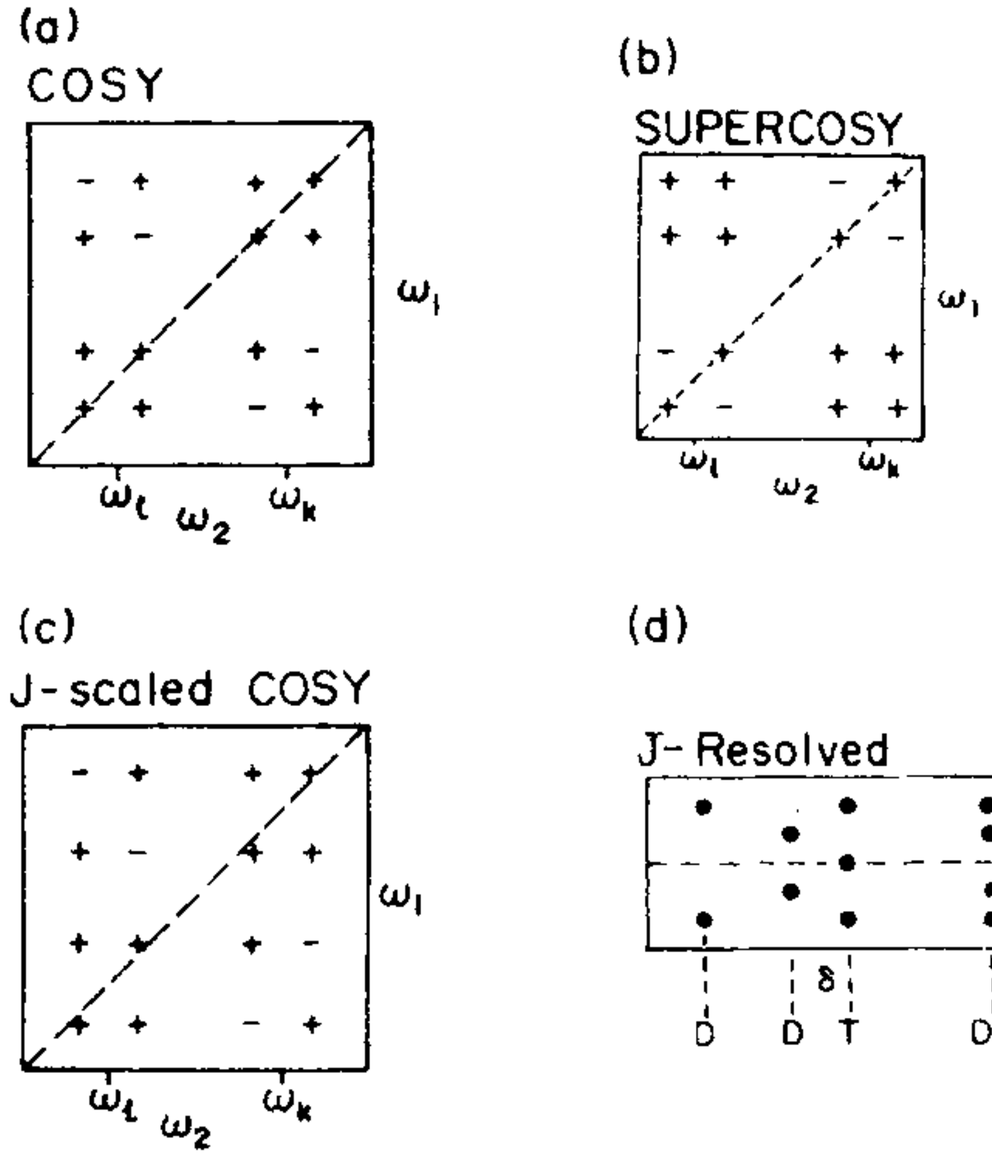

Figure 2. Schematic spectra. In *J*-resolved experiment D = doublet, T = triplet and DD = doublet of doublet. ω_k and ω_l are rotating frame Larmor frequencies of spins *k* and *l* respectively.

above. For two spins, when the delay parameter Δ is set equal to $1/4J$, the appearance of the 2D spectrum is shown in figure 2b. Now, it is seen that the cross peaks have all positive components while the diagonal peak components acquire positive and negative signs. This results in an improved cross-peak intensity and at the same time, the diagonal peaks have lower intensities. If the above mentioned condition on Δ is not satisfied (which usually happens since there may be several coupling constants in the system), there will be a partial enhancement of cross-peak intensities. Thus it is advantageous to give short delays of the order of 0.01–0.02 sec so that most of the cross peaks in the spectrum appear more prominently than in the COSY spectrum and simultaneously the diagonal peaks appear with lower intensities. Consequently, the dynamic range problem is also partially solved. Further, the fact that Δ depends on coupling constants *J* suggests that the experiment can be tuned to enhance particular cross peaks. This has been utilized to observe long range coupling correlations in peptides and oligonucleotides[14–16].

Thus it is clear that the delay Δ is a crucial parameter in the SUPER COSY pulse scheme. It is of course important that $\Delta << T_2^*$ (transverse relaxation time), so that there is observable magnetization during the detection period t_2. This condition, sometimes, proves to be a disadvantage since, in large biological systems T_2^* values are less than 0.05 sec and large delays like $\Delta = 0.05$ which correspond to a commonly occurring *J* value of 5 Hz cannot be afforded.

The pulse scheme C (J-scaled COSY)[17] is a further improvement to overcome the sensitivity problems encountered in the SUPERCOSY scheme. Here, the *J*-value is artificially enhanced during the evolution period by allowing the spin system to evolve for a longer time under the influence of the coupling part of the total Hamiltonian, than it does under the influence of the Zeeman part of the Hamiltonian. Thus there is a greater separation, along the ω_1-axis, between the + and the − components of the cross peaks. Consequently, under the given resolution conditions, the cancellation of component intensities is reduced and the cross peaks appear more pronounced. Due to the absence of fixed delays, losses due to transverse relaxation are minimized and sensitivity is substantially higher as compared to the SUPERCOSY scheme. Figure 2c shows the appearance of the *J*-scaled spectrum in the case of a two-spin system. It is important to mention here that the resolution along ω_1-axis is usually poorer than that along the ω_2-axis. Therefore, it is generally sufficient to scale the *J*-values along the ω_1-axis. For special experiments, such as for observation of long-range coupling correlation, it becomes necessary to use a delay period after the second 90° pulse to convert + − signals to + + signals along the ω_2-axis. The *J*-scaled COSY experiment has been used to observe coupling correlations corresponding to very small *J*-values (0.3 Hz) in oligonucleotides[16].

Pulse scheme D (relayed COSY[18]) is an extension of the COSY principle to observe coupling correlations between spins which are not directly coupled, but have a coupling partner. For exam-

ple, in a linear 3-spin system *A-M-X*, *A-X* coupling correlations can be observed although $J(AX)$ is zero. Magnetization is transferred sequentially $A \rightarrow M$ and $M \rightarrow X$. This is helpful in resolving ambiguities arising from overlap of signals. For example, similar COSY patterns will be observed in the case of an *AMX* spin system and in a mixture of two 2-spin systems *AM* and *M'X* when *M* and *M'* have identical chemical shifts. But in the relayed COSY *A-X* correlations will be seen only for the *AMX* spin system.

Pulse scheme E (COSS) is aimed at improving the resolution in the 2D-*J*-correlated spectra[19,20]. The idea here is to scale up the chemical shifts along the ω_1-axis while the coupling constants are left unaffected. Consequently the separation between the different cross peaks is increased resulting in a resolution enhancement. This technique also achieves some amount of sensitivity enhancement in the cross peaks. Figure 3 shows a comparison of COSY and COSS to illustrate the resolution enhancement in the latter.

While the pulse schemes *A-E* are helpful in identifying *J*-coupling correlations, scheme F (NOESY)[21,22] shows a completely different type of correlations namely dipolar coupling correlations. The NOESY spectrum looks very similar to the *J*-correlated spectra described above, but the cross peaks now identify spins which are closeby in space and exchange magnetization via dipolar interactions. Thus the intensities of the cross peaks reflect the distance between the interacting spins. This fact can be utilized for determination of structure in solution.

Finally pulse scheme G[23] is designed for accurate measurement of ^1H–^1H coupling constants. The appearance of the spectrum is shown in figure 2d. Cross-sections along the ω_1-axis through the peaks show the multiplets and thus directly give coupling constant information. Since the ω_2-axis is devoid of the coupling constants, the resolution along this axis is greatly enhanced and spins which have very nearly identical chemical shifts can be resolved.

In addition to the schemes described above certain other schemes namely ^{31}P-^1H correlations[24] and double quantum spectroscopy[25] have also been occasionally used in the literature.

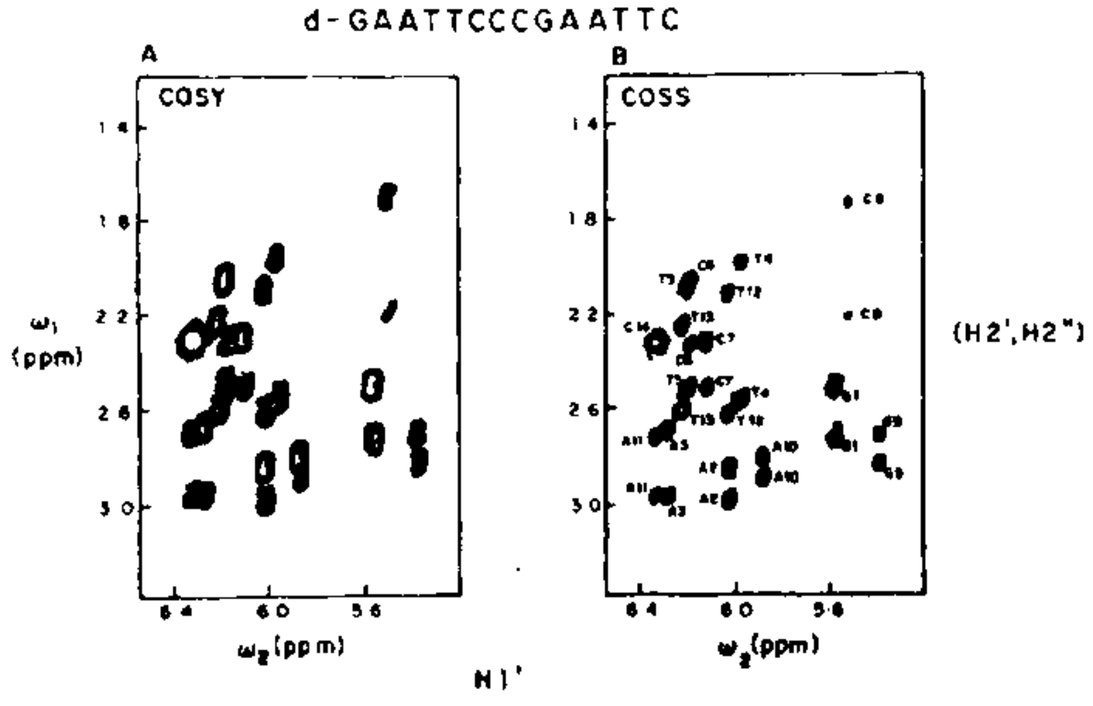

Figure 3. Portions of 500 MHz COSY and COSS spectra of *d*-GAATTCCCGAATTC. Shift scaling factor in COSS is 1.5.

RESONANCE ASSIGNMENTS IN NUCLEIC ACIDS

Resonance assignment is the first step in any endeavour and we shall be concerned only with ^1H NMR assignments. From the NMR point of view, the protons in nucleic acids can be grouped into four categories; (i) exchangeable NH protons of the bases which resonate between 10–16 ppm downfield from 3-trimethylsilyl-(2,2,3,3-^2H)propionate (TSP), (ii) exchangeable NH and non-exchangeable base protons resonating between 7–9 ppm downfield from TSP, (iii) non-exchangeable sugar protons which appear between 2–6.5 ppm and finally (iv) methyl protons of thymines which resonate between 0.5–2 ppm downfield of TSP. In order to observe the NH protons, experiments will have to be carried out in H_2O, whereas the other protons can be observed in D_2O solutions. We shall be mainly concerned with non-exchangeable protons since they are easy to observe and provide almost 90–95% information on the solution structures.

Assignment of the various resonances to individual protons can be obtained by using the *J*-correlated and NOESY techniques discussed in the previous section. The strategies involved have been published[26–31] and the procedure consists of basically two steps. In the first stage

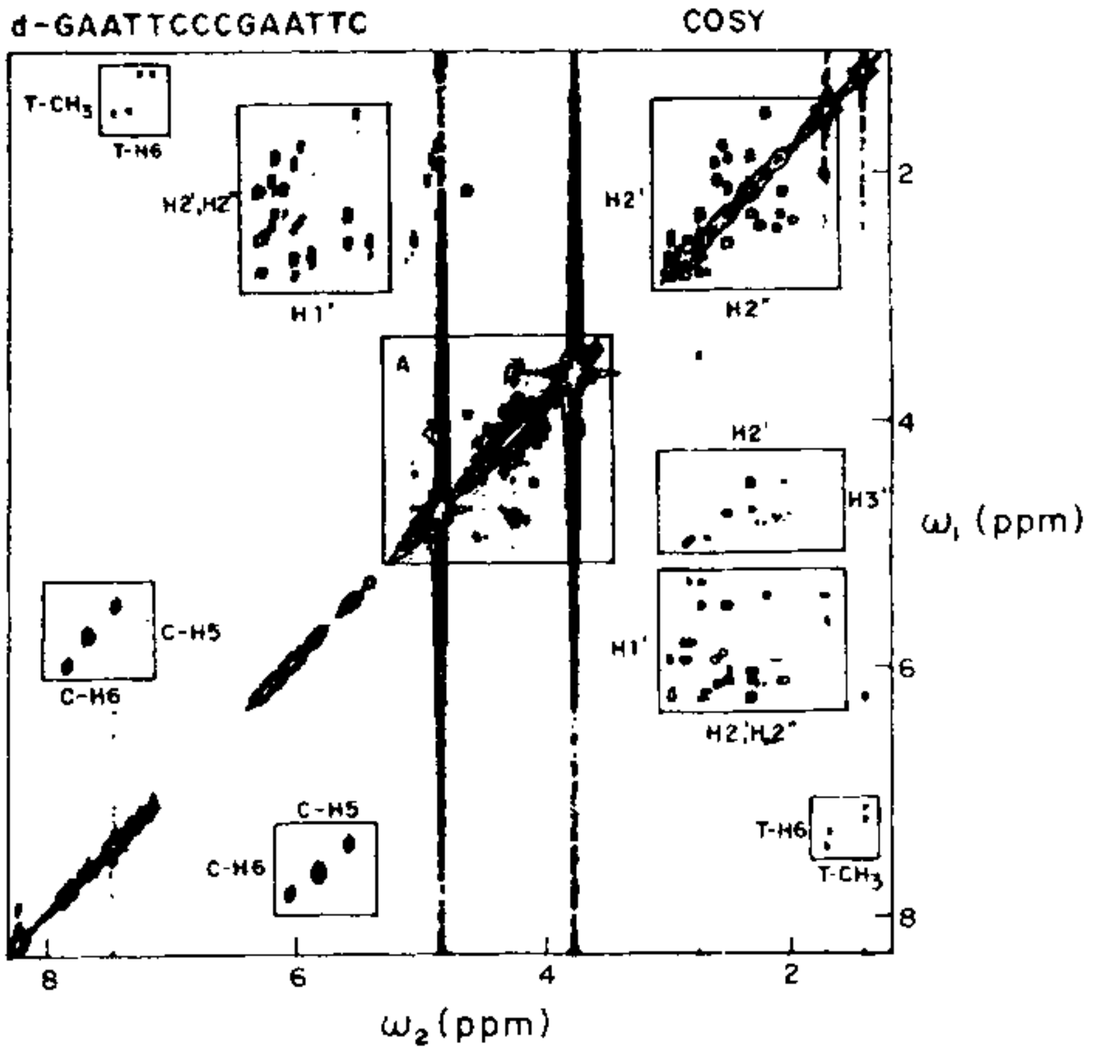

Figure 4. 500 MHz COSY spectrum of *d*-GAATTCCCGAATTC, showing identification of various cross peak regions.

the *J*-correlated spectra are used to identify networks of coupled spins. In the second stage, the spin systems identified are assigned to particular nucleotides along the sequence of the molecule, by making use of the NOESY spectrum.

Figure 4 shows a 500 MHz COSY spectrum of a double helical oligonucleotide having the sequence;

5′–*d*–GAATTCCCGAATTC–3′.

This spectrum shows all the 14 H1′–(H2′, H2″), H2′–H2″, and H2′–H3′ cross peaks. H2″–H3′ cross peaks are not seen and this has important structural implications which will be discussed later. The central box A in the spectrum contains peaks arising from H3′, H4′, H5′ and H5″ protons. Many of these are very close to the diagonal and are not well resolved. The spectrum also shows H5––H6 cross peaks of cytosine and H6––CH_3 cross peaks of the thymine nucleotides. The spectrum shown in figure 4 allows identification of most of the sugar spin systems. In a few cases ambiguities arise due to the overlap of H3′ protons and H2′ protons of two nucleotides. These ambiguities are resolved by the remote H1′––H3′ and H2′–H4′ connectivities in the relayed-COSY spectrum shown in figure 5.

The *J*-correlated spectra, however, do not show any correlation between the base protons and the respective sugar ring protons. Thus from these spectra alone it is not possible to assign the spin systems to individual nucleotide units along the sequence of the molecule. For this purpose the NOESY spectrum which shows distance correlations becomes useful. The NOESY spectrum contains cross peaks between all those protons which are less than 4 Å apart. It is thus obvious that appearance of the NOESY spectrum is crucially dependent on the 3D structure of the nucleic acid fragment. Figure 6 shows a NOESY spectrum of a double helical oligonucleotide having the sequence,

5′––*d*–GGATCCGGATCC––3′.

The spectrum shows a number of cross peaks between the base protons and the sugar protons. These can be classified into two categories (i) those which arise from protons in the same nucleotide unit and (ii) those which arise from

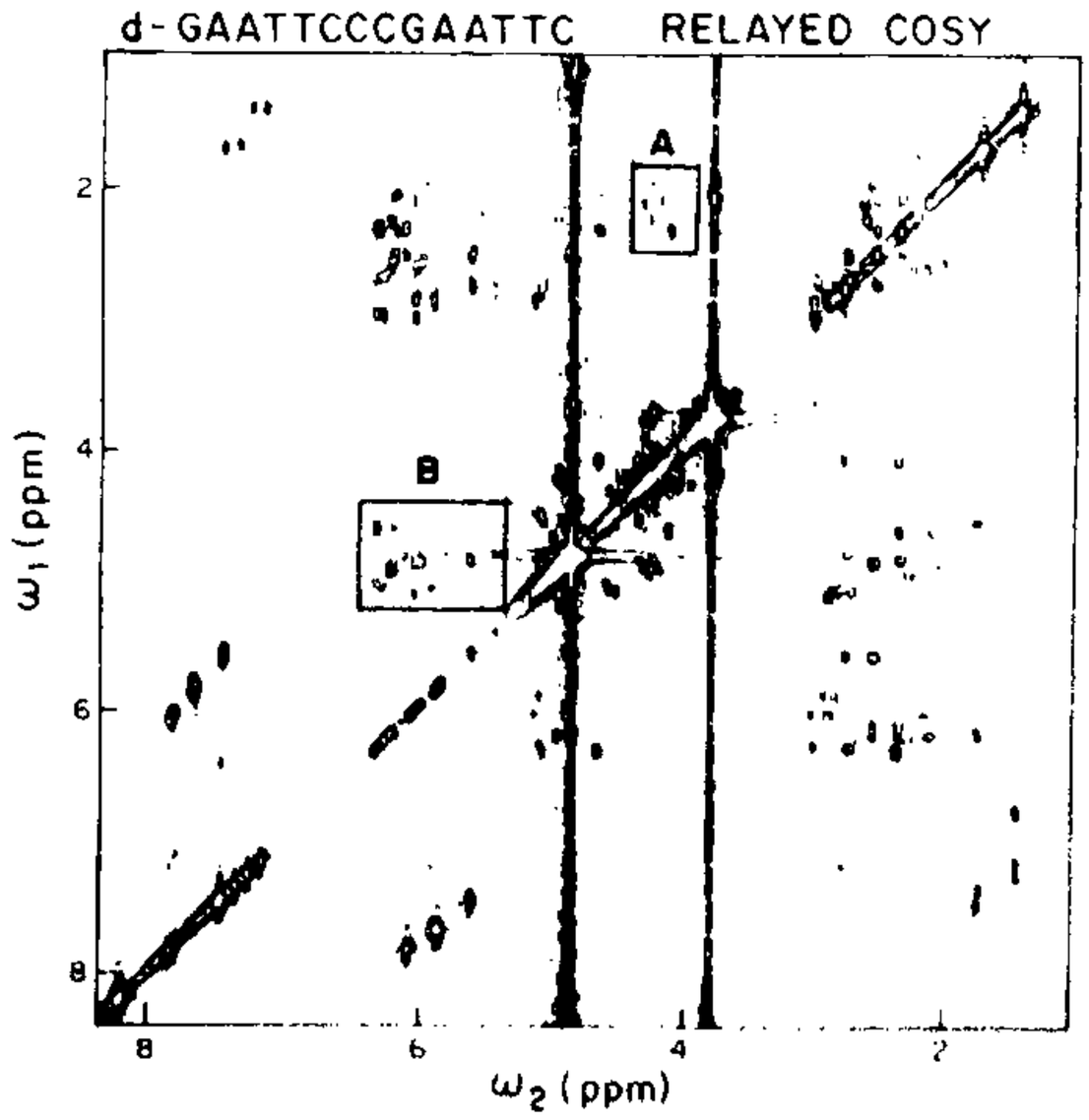

Figure 5. 500 MHz relayed COSY spectrum of *d*-GAATTCCCGAATTC in D_2O. The boxes show the remote connectivities, H1′-H3′ (B) and H2′–H4′ (A).

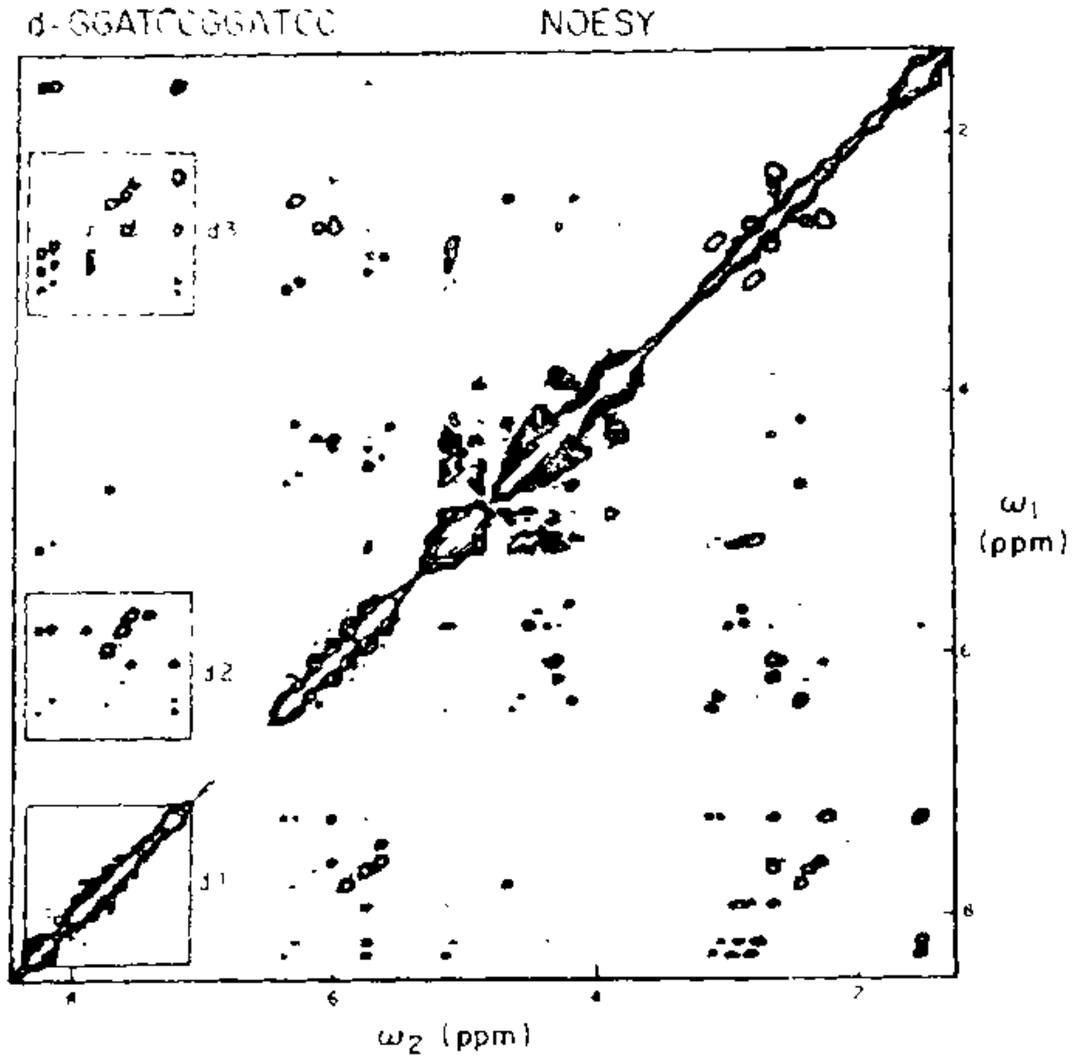

Figure 6. 500 MHz NOESY spectrum of *d*-GGATCCGGATCC showing cross peak regions of sequential d1, d2 and d3 connectivities.

protons on adjacent nucleotide units. The latter allow sequential assignment of the protons to individual nucleotide units. The sequential NOESY connectivities observable in right-handed DNA structures are of three types: (i) $(base)_i$--- $(base)_{i\pm1}$ (d1), (ii) $(base)_i$--- $(H1')_{i-1}$ (d2), (iii) $(base)_i$--- $(H2'')_{i-1}$ (d3). The latter two are schematically indicated in figure 7b. Since the chemical shifts of base, H1′ and H2″ protons are very different, the three sets of cross peaks appear at distinctly different regions of the NOESY spectrum (figure 6). While the d1 connectivities help in sequential assignment of base protons only, the d2 and d3 connectivities enable assignment of both sugar protons and base protons. The sequential assignment using d2 connectivity would proceed as; $(base)_i$---- $(H1')_{i-1}$---- $(base)_{i-1}$---- $(H1')_{i-2}$---- etc. Similarly, assignment via d3 connectivity would proceed as; $(base)_i$----- $(H2'')_{i-1}$----- $(base)_{i-1}$ ----- $(H2'')_{i-2}$ etc. Sometimes one may also see connectivities via the H2′ protons. In certain cases, when $(base)_i$ ---- $(H2'')_i$ NOEs are not seen, both H2′ and H2″ protons can be used simultaniously; the assignment would proceed as $(base)_i$ ---- $(H2'')_{i-1}$

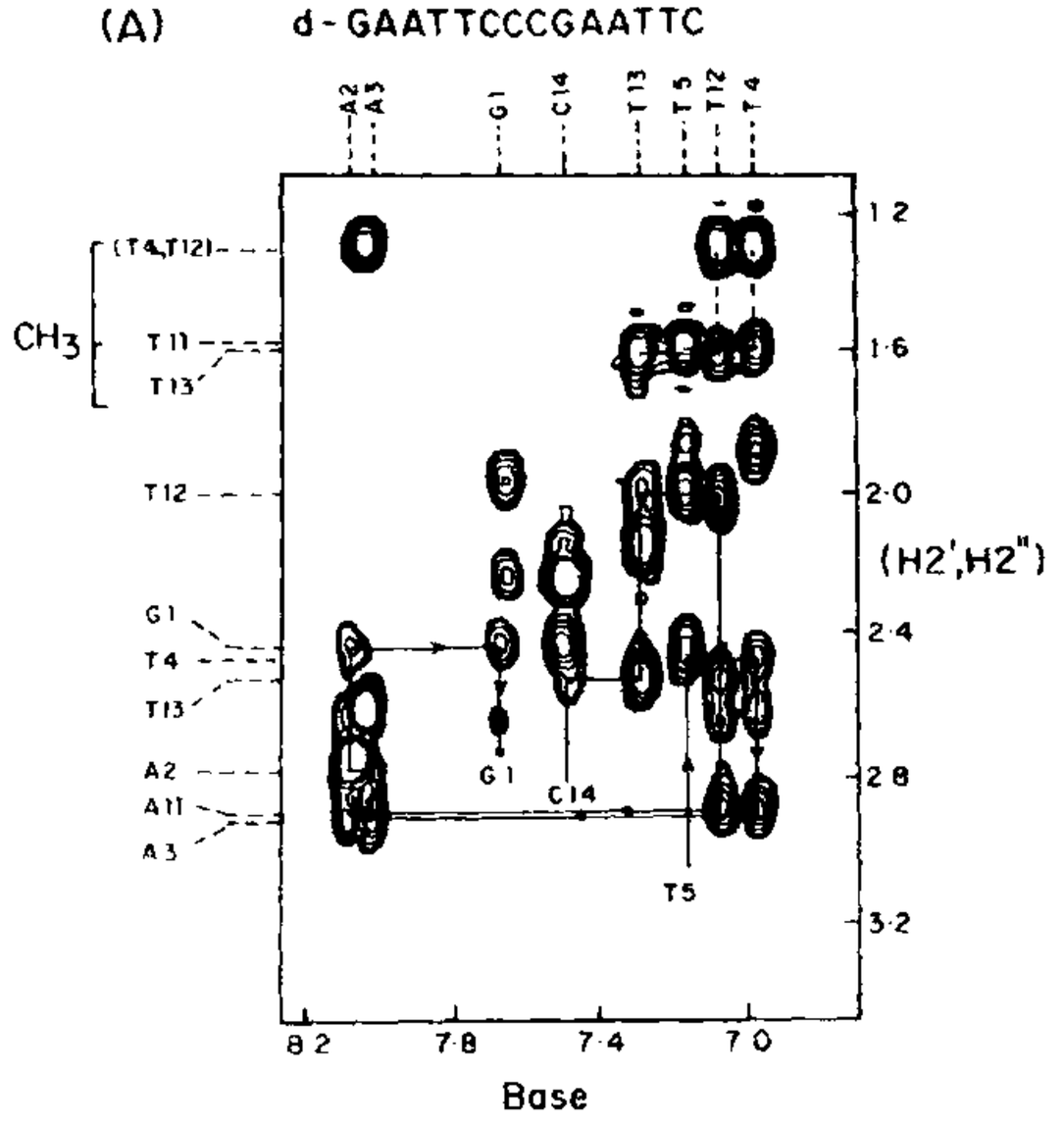

Figure 7. (A) Sequential d3 connectivities in *d*-GAATTCCCGAATTC. (B) Dinucleotide fragment depicting the various sequential connectivities. Thick arrows indicate internucleotide NOEs (sequential connectivities) and thin arrows show intranucleotide NOEs. The sequential d1 connectivities (see text) are not drawn to avoid overcrowding in the figure.

$---(H2')_{i-1}---(base)_{i-1}---(H2'')_{i-2}$. Generally more than one type of connectivities can be observed. The d3 connectivities are usually stronger than d2 connectivities and are also characteristic of right-handed structures.

Using the strategies discussed above, complete resonance assignments have been obtained in four oligonucleotides namely, *d*-GGATCCGGATCC (I), *d*-GAATTCGAATTC (II), *d*-CGCGCGCGCGCG (III) and *d*-GAATTCCCGAATTC (IV). Details of these are being published elsewhere[32-34]. Figure 7a shows illustrative d3 connectivities via H2″ protons observed in molecule IV.

In the case of left-handed Z type of structures[35] the above strategies do not work and a different set of sequential connectivities will have to be used[26]. Work is in progress to examine the possibility of other left-handed structures in solution and to devise suitable assignment strategies.

SOLUTION STRUCTURE OF NUCLEIC ACIDS

The successful sequential assignment procedure, already provides important clues to the overall structure of the nucleic acid fragment under study. For example, all the molecules I–IV mentioned above have been found to possess right-handed structures and are in the double helical form. However, in order to define the structure more precisely, the sugar geometry, the glycosidic dihedral angle and the six dihedral angles in the backbone have to be specified. We have recently discussed the procedures for determination of sugar geometries and the glycosidic dihedral angle using the 2D NMR techniques[26, 27, 32].

Sugar geometries of the individual nucleotide units can be determined by measuring the various 3-bond ^1H–^1H coupling constants in the rings. The coupling constants are related to the relevant dihedral angles by the Karplus type relation[36].

$$J = 10.2\cos^2\phi - 0.8\cos\phi$$

where ϕ is the dihedral angle. Figure 8 shows the variation of ^1H–^1H coupling constants as a function of the pseudorotation parameter P[37]. The classical ring conformations corresponding to particular values of P are also indicated in the figure. Thus from a knowledge of the several coupling constants, the sugar geometry can be uniquely determined.

The ^1H–^1H coupling constants can be accurately measured using 2D–*J*–resolved experiment (figure 1G). The technique, however, has sensitivity problems and in large oligonucleotides it is difficult to obtain good spectra with intense cross peaks. We have recently shown that even the COSY or COSS spectra can be used for identification of sugar geometry[32]. This relies on the fact, the intensities of cross peaks in COSY or COSS spectra are crucially dependent on *J*-values when the spectra are recorded with poor digital resolution. Cross peaks involving *J*-values of less than 3 Hz are usually not observed. Thus different sugar geometries produce different patterns of cross peaks in the COSY/COSS spectra. For example, H2″–H3′ cross peaks will not be seen for C2′-endo sugar geometry, but will be strong for C3′-endo conformation. On the basis of these principles, we have observed that *d*-GAATTCGAATTC (II) and *d*-GAATTCCCGAATTC (IV) have 70% nucleotides in O1′-endo conformation, in contrast to the most popular C2′-endo or C3′-endo geomet-

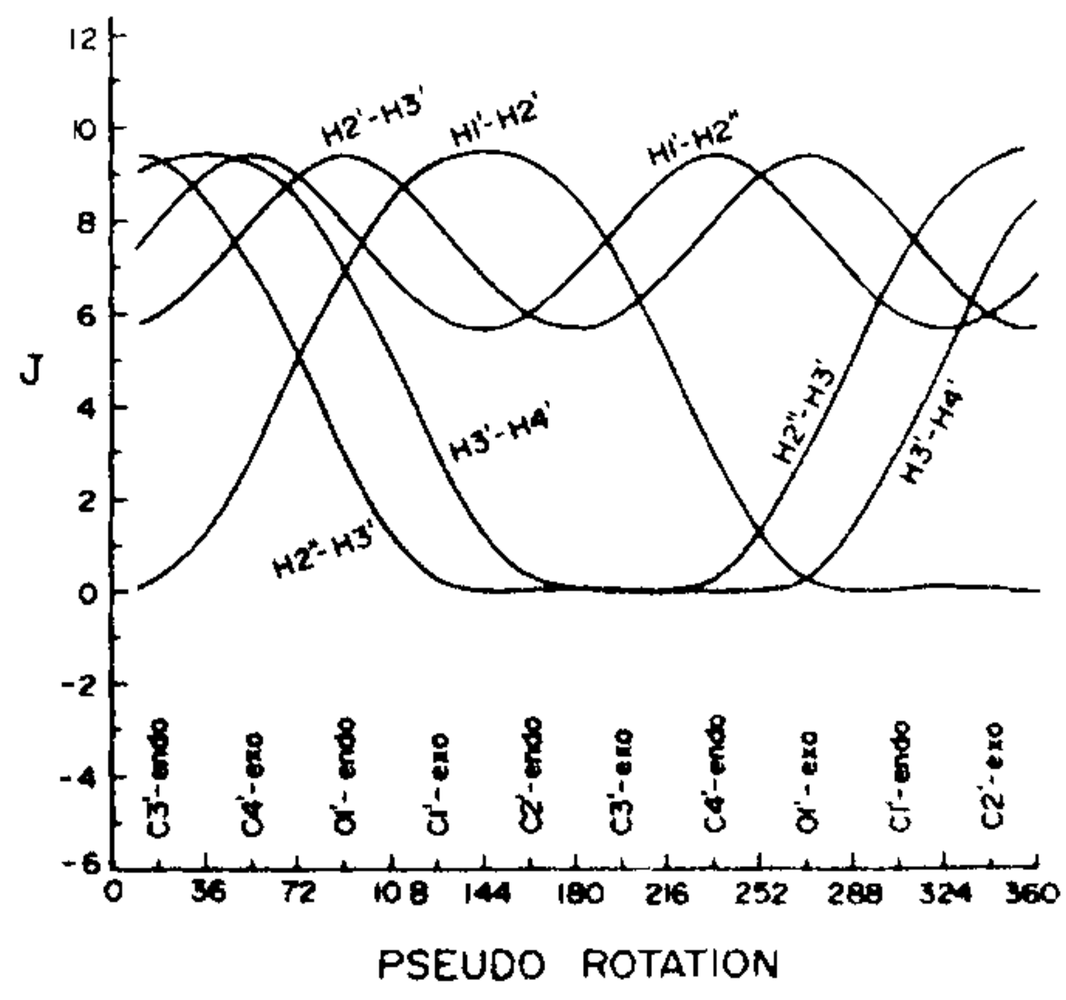

Figure 8. Variation of the vicinal coupling constants in the *d*-ribose ring as a function of the ring geometry.

ries observed in smaller fragments of nucleic acids. The sugar geometries have been determined all along the sequence in all the four molecules I–IV, and it has been found that the mismatch region in IV exhibits sugar conformations[32, 33] different from the rest of the nucleotides. This variation may facilitate looping out of the helix in the centre.

Information about the glycosidic dihedral angle (χ) can be obtained by monitoring the relative intensities of the NOESY cross peaks, base $(H8/H6)_i \ldots\ldots (H1')_i$ and base $(H8/H6)_i \ldots\ldots (H2')_i$. The former are strong if χ is in the syn-domain, while the latter are strong in the anti-domain of the dihedral angle. All the molecules mentioned above possess χ values in the anti domain.

As regards the backbone, dihedral angles C3′-C4′-C5′-O5′, C4′-C3′-O3′-P and C4′-C5′-O5′-P can be determined by measuring the H4′-(H5′-H5″), (H3′-P) and (H5′,H5″)-P, 3-bond coupling constants. Two dimensional ^{31}P-^{1}H correlated experiments wherein all the ^{31}P-^{1}H coupling constants are retained will be useful for the latter two values. Efforts along this direction are in progress in our laboratory. With regard to the remaining C3′-O3′-P-O5′ and O3′-P-O5′-C5′ dihedral angles, there is no direct method of evaluation. Estimates of base-base stacking can be used to derive this information in an indirect manner.

CONCLUSIONS

We have described how 2D NMR can give a detailed structural information, so much so that, one may loosely call it as 'crystallography in solution.' The presence of evolution and mixing periods in the 2D NMR general scheme provides a large flexibility in manoeuvering with spin systems and thus in obtaining a variety of information unobtainable otherwise. With all these developments, it is becoming increasingly evident that nucleic acids show a wide range of structures than were thought to be exhibiting before. Consequently it is anticipated that the nucleic acids also play a significant role in recognition phenomena. Clues to this effect have already started emerging in the literature. We have observed different sugar geometries at the recognition sites of restriction enzymes Bam HI and Eco RI in *d*-GGATCCGGATCC and *d*-GAATTCGAATTC[26, 27, 32] respectively.

ACKNOWLEDGEMENTS

The author has collaborated with several colleagues, namely Mr. M. Ravi Kumar, Mrs. Anu Sheth, Dr K. V. R. Chary, and Prof. G. Govil in the NMR work on nucleic acids reviewed in this article. Dr H. T. Miles of National Institute of Health, U.S.A. has synthesized and provided the deoxy oligonucleotides. The SUPERCOSY technique was developed in collaboration with Prof. Anil Kumar and Mr. K. Chandrasekhar of Indian Institute of Science, Bangalore. The *J*-scaled COSY and COSS were developed in collaboration with Dr K. V. R. Chary, Mr. M. Ravi Kumar and Mrs. Anu Sheth in our group. The NMR spectra were recorded on the Bruker AM-500 spectrometer at the FTNMR-National Facility and the help provided is gratefully acknowledged.

9 January 1986; Revised 4 March 1986

1. Govil, G. and Hosur, R. V., *Conformation of biological molecules: New results from NMR*. Springer Verlag, Berlin, 1982.
2. Tewari, R., Nanda, R. K. and Govil, G., *J. Theor. Biol.*, 1974, **46,** 229.
3. Pullman, B. and Saran, A., *Prog. Nucl. Acids Res. Molec. Biol.*, 1976, **18,** 215.
4. Sundaralingam, M., *Biopolymers*, 1982, **7,** 821.
5. Sasisekharan, V., Bansal, M., Brahmachari, S. K. and Gupta, G., In: *Biomolecular stereodynamics* (eds) R. H. Sarma, Adenine press, New York, 1981, p. 123.
6. Wagner, G. and Wuthrich, K., *J. Mol. Biol.*, 1982, **155,** 347.
7. Hosur, R. V., Wider, G. and Wuthrich, K., *Eur. J. Biochem.*, 1983, **130,** 497.
8. Wuthrich, K., *Biomedical Res.*, 1984, **5,** Supplement, 151.
9. Williamson, M. P., Havel, T. F. and Wuthrich, K., *J. Mol. Biol.*, 1985, **182,** 295.

10. Zuiderweg, E. R. P., Billeter, M., Boelens, R., Scheek, R. M., Wuthrich, K. and Kaptein, R., *FEBS Lett.*, 1984, **174,** 243.
11. Jeener, J., Ampere Summer School, Basko, Polje, Yugoslavia, 1971.
12. Aue, W. P., Bartholdi, E. and Ernst, R. R., *J. Chem. Phys.*, 1976, **64,** 2229.
13. Anil Kumar, Hosur, R. V. and Chandrasekhar, K., *J. Magn. Reson.*, 1984, **60,** 143.
14. Hosur, R. V., Chary, K. V. R., Anil Kumar and Govil, G., *J. Magn. Reson.*, 1985, **62,** 123.
15. Mayor, S. and Hosur, R. V., *Magn. Reson. Chem.*, 1985, **23,** 470.
16. Gundhi, P., Chary, K. V. R. and Hosur, R. V., *FEBS Lett.*, 1985, **191,** 92.
17. Hosur, R. V., Chary, K. V. R. and Ravikumar, M., *Chem. Phys. Lett.*, 1985, **116,** 105.
18. Eich, G., Bodenhausen, G. and Ernst, R. R., *J. Am. Chem. Soc.*, 1982, **104,** 3731.
19. Hosur, R. V., Ravikumar, M. and Sheth, A., *J. Magn. Reson.*, 1985, **65,** 375.
20. Ravikumar, M., Sheth, A. and Hosur, R. V., *J. Magn. Reson.* (in press).
21. Jeener, J., Meier, B. H., Bachmann, P. and Ernst, R. R., *J. Chem. Phys.*, 1979, **71,** 4546.
22. Anil Kumar, Wuthrich, K. and Ernst, R. R., *Biochem. Biophys. Res. Commun.*, 1980, **95,** 1.
23. Aue, W. P., Karhan, J. and Ernst, R. R., *J. Chem. Phys.*, 1976, **64,** 4226.
24. Pardi, A., Walker, R., Rapoport, H., Wider, G. and Wuthrich, K., *J. Am. Chem. Soc.*, 1983, **105,** 1652.
25. Vandeven, F. J. M., Haasnoot, C. A. G. and Hilbers, C. W., *J. Magn. Reson.*, 1985, **61,** 181.
26. Hosur, R. V., Ravikumar, M., Roy, K. B., Tan Zu Kun, Miles, H. T. and Govil, G., In: *Magnetic resonance in biology and medicine* (eds) G. Govil, C. L. Khetrapal and A. Saran, Tata McGraw Hill, New Delhi, 1985, p. 243.
27. Ravikumar, M., Hosur, R. V., Roy, K. B., Miles, H. T. and Govil, G., *Biochemistry*, 1985, **24,** 7703.
28. Clore, G. M. and Gronenborn, A. M., *FEBS Lett.*, 1985, **179,** 187.
29. Gronenborn, A. M. and Clore, G. M., *Prog. NMR. Spectrosc.*, 1985, **17,** 1.
30. Kearns, D. R., *Biochemistry*, 1984, **23,** 791.
31. Govil, G., Kumar, N. V., Ravikumar, M., Hosur, R. V., Roy, K. B. and Miles, H. T., *J. Biosci.*, 1985, **8,** Supplement 3, 645.
32. Hosur, R. V., Ravikumar, M., Chary, K. V. R., Sheth, A., Govil, G., Tan Zu Kun and Miles, H. T., *FEBS Lett.*, (in press).
33. Chary, K. V. R., Hosur, R. V., Govil, G., Tan Zu Kun and Miles, H. T., *Biochemistry*, (submitted).
34. Sheth, A., Ravikumar, M., Hosur, R. V., Govil, G. and Miles, H. T., *Biopolymers*, (submitted).
35. Wang, A. H. J., Quigley, G. J., Kolpak, F. J., Crawford, J. L., Van Boom, J. H., Van der Marel, G. and Rich, A., *Nature (London)*, 1979, **282,** 680.
36. Davies, D. B., *Prog. NMR. Spectrosc.*, 1978, **12,** 135.
37. Altona, C. and Sundaralingam, M., *J. Am. Chem. Soc.*, 1972, **94,** 8205.